

# Entropic competition between knots and slip-links

Roya Zandi,<sup>1,2</sup> Yacov Kantor,<sup>3</sup> and Mehran Kardar<sup>2</sup>

<sup>1</sup>*Department of Chemistry and Biochemistry, UCLA,  
Box 951569, Los Angeles, California, 90095-1569*

<sup>2</sup>*Department of Physics, Massachusetts Institute of Technology, Cambridge, MA 02139, USA*

<sup>3</sup>*School of Physics and Astronomy, Raymond and Beverly Sackler  
Faculty of Exact Sciences, Tel Aviv University, Tel Aviv 69978, Israel*

(Dated: October 9, 2017)

Using canonical Monte Carlo simulations, we introduce a new numerical procedure for comparing the entropic exponents of polymers with different constraints and/or topologies. Setting up competitions between polymer segments which can exchange monomers according to their free energies, we obtain the universal exponents of partition functions, independently of any knowledge of the non-universal part. The method is successfully tested for closed polymer loops decorated with sliding rings. We also investigate the entropic exponents of loops with a fixed knot type, in which case we are limited by strong finite-size effects.

## I. INTRODUCTION AND SUMMARY

A long flexible polymer chain can assume an enormous number of configurations; thus, the conformations of polymers are best described statistically. Despite the microscopic distinctions which exist among different polymers, at large length scales many generic properties are independent of the details of specific polymer structure and thus are “universal.” [1] The understanding and characterization of this universal behavior has led to great advances in the statistical treatment of polymers. Polymers in good solvents have been modeled by self-avoiding walks (SAWs), which are in turn mapped to a magnetic system at its critical point [1]. Renormalization group techniques then allow a variety of polymer properties to be calculated analytically [1, 2]. On the experimental front, advances in manipulation and imaging of single molecules have provided new impetus for studies of polymers [3]. With these micromanipulation techniques, it is now possible to explore a wide variety of physical properties of polymers, and thus to test models and theoretical predictions at the level of a single chain.

In many circumstances, the number of configurations of a polymer grows with its length  $\ell$ , as

$$w(\ell) \simeq A\mu^\ell \ell^{-c} [1 + B\ell^{-\Delta} + \dots]. \quad (1)$$

In the above equation, the connectivity constant  $\mu$ , is a non-universal quantity which depends on the microscopic features of the chain, but (like a free energy density) remains the same for different boundary and topological constraints [1]. By contrast,  $c$  is a *universal* exponent, which is independent of the microscopic characteristics of the polymer, but which does depend on the dimensionality, and on global boundary and topological constraints. For example, in the case of a closed loop,  $c = d\nu$ , where  $d$  is the dimensionality of space, and  $\nu$  is the exponent relating the typical spatial extent of a polymer to its length by  $R \sim \ell^\nu$ . (In  $d = 3$ , for polymers with self-avoiding interactions  $\nu \approx 0.588$  [1, 4].) In Eq. (1), we have anticipated subleading corrections to the leading asymptotic

behavior at large  $\ell$ , indicated by so-called corrections to scaling in the square brackets. Renormalization group calculations suggest that the exponent  $\Delta$  is universal, while the amplitude  $B$  is case-specific [2].

Numerical determination of a power-law correction to the leading exponential behavior is rather cumbersome. It is usually accomplished by examining a generating function  $f(z) = \sum_\ell \ell^g w(\ell) z^\ell$ , with a conveniently chosen value of the free parameter  $g$ . The function  $f(z)$  is usually singular at  $z = 1/\mu$  [5], and the details of this singularity determine the exponent  $c$  appearing in Eq. 1. This can be done either by examining a finite amount of terms in series expansions, using  $w(\ell)$  extracted from exact enumeration studies, or by performing grand-canonical Monte Carlo (MC) studies of the polymer with weight determined by  $\ell^g z^\ell$  for several values of  $z$ , as was done in Refs. [6, 7].

Here, we propose a method for calculating the universal exponent  $c$  in the number of configurations, without the need to account for the leading non-universal exponential growth  $\mu^\ell$ . Our procedure is best suited for the evaluation of the exponent  $c$  when the polymer is constrained in various manners, a situation that occurs physically when a polymer can move from one regime to another. Using canonical Monte Carlo simulations, we directly compare the *relative* number of configurations by setting up an ensemble in which two segments of a polymer can exchange monomers. A pair of monomers belonging to two different segments does not interact, while the monomers in the same segment repel each other. Each segment is subject to its own set of global constraints. The total number of monomers is fixed to  $L$ , while in any given configuration the two segments have  $\ell$  and  $L - \ell$  monomers, respectively. According to Eq. (1), in the asymptotic limit, the number of configurations of such a system is

$$w(\ell, L) = A\ell^{-c_1} (L - \ell)^{-c_2}, \quad (2)$$

where  $c_1$  and  $c_2$  are the exponents characterizing each segment; the prefactor  $A$  is independent of  $\ell$ . Assuming

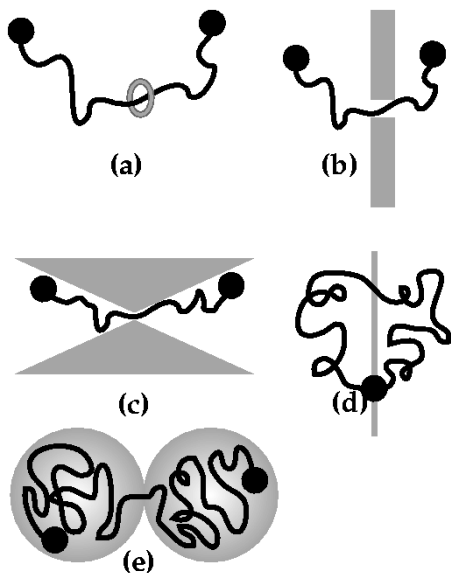


FIG. 1: Examples of possible applications of “entropic competition:” (The universal power-law exponents depend on the boundary condition of the system.) (a) is appropriate for calculation of the exponent  $\gamma$  which describes open linear polymers. Note that the two segments of the chain do not interact with each other. (b) is good for calculation of the exponent  $\gamma_1$ , (c) for a wedge, (d) for exponent  $\gamma_{11}$ , and (e) for a chain attached at one end to the interior surface of a sphere.

that the asymptotic limit has been reached, fitting the histogram of  $\ell$  should provide the exponents  $c_1$  and  $c_2$ .

This method, which we call “entropic competition,” can in principle be applied to several physical circumstances, some of which are depicted in Fig. 1. For example, one can extract the entropic exponents of linear chains by threading them through a hole, and making the first and last monomers of the chain bigger than the size of the hole such that the chain can diffuse back and forth without wandering away (Fig. 1a). A key point in this set-up is that the two parts of the chain are not allowed to interact with each other. By examining the probability of having a segment of size  $\ell$ , which is proportional to  $\ell^{\gamma-1}(L-\ell)^{\gamma-1}$ , one can extract the entropic exponent of linear chains, known as  $\gamma$  [8]. If, instead of threading a chain through a hole, we divide the chain into two parts by a rigid wall and let the two parts of the chain exchange monomers at the wall (a process called translocation), we can extract the entropic exponent which is called  $\gamma_1$  [8] (Fig. 1b). Other potential applications are to the calculation of entropic exponents of linear polymers in the presence of a wedge, or inside a spherical shell (Figs. 1(c, e)). The latter case is particularly relevant to the translocation of DNA through spherical capsids and has been the subject of intense research[9]. “Entropic competition” is especially appropriate for calculation of the entropic exponent  $\gamma_{11}$ , related to the polymers with two ends anchored to a surface [8]. In this case, by fixing one monomer of a ring on a wall and letting the two seg-

ments of the ring on the two sides of the wall exchange monomers with each other at any point on the wall, we can extract the entropic exponents of chains with two ends restricted to move on a surface (Fig. 1e). The latter is of renewed interest due to potential relevance to a new class of physical gels obtained from triblock copolymers anchored to fluid membranes at each end [10].

The calculation of entropic exponents using “entropic competition” is not solely restricted to open polymers. One can divide a ring into two loops with the use of a ‘hole’ connecting two separate spaces, and a monomer which is fixed in position, as illustrated in Fig. 2. In Sec. II we employ this system to calculate the probability distribution of two *non-interacting* self-avoiding (SA) loops of lengths  $\ell$  and  $L - \ell$ , which can freely exchange monomers. If the two polymer segments have the same topology and boundary conditions, as in the aforementioned case, then the exponents  $c_1$  and  $c_2$  of Eq. (2) are equal and one can directly find the entropic exponents by fitting the probability distributions resulting from simulations to Eq. (2).

The entropic exponent can in fact be modified in a systematic manner by decorating polymer loops with sliding rings. We investigate the effect of sliding rings on the number of configurations of closed chains in Sec. III. We assume that the size of a ring is the same as that of one monomer. In this situation, the presence of a ring increases the number of configurations of the loop by a factor of  $\ell$  (the number of monomers on the loop where the ring can slide). Once again we examine the accuracy of “entropic competition” by comparing the results of the simulations with analytical expectations, and find an excellent agreement between them.

Introduction of the “entropic competition” method was motivated by its potential application to *knots*. The influence of a knot on the entropy of polymers has been the subject of interest for some time [6, 7, 11, 12]. In Sec. IV we study knotted polymers. We overview the current hypothesis regarding the number of configurations of a knotted polymer. We numerically study several related models and observe that the presence of knots changes the number of configurations. Furthermore, we numerically calculate the probability distribution of two loops with one trefoil knot on each side and find that it is completely different from that of two loops with one ring on each side. This may well be an indication of the importance of finite-size effects in knots, as the two cases are conjectured to be similar in the limit of very long chains.

Finally, in Sec. V, we observe the “competition” between a knot and rings by placing a knot on one loop and rings on the other loop. In our simulations, the knot pulls the chain much harder than a single ring, possibly due to finite-size effects. For polymers in the range of a few hundred monomers, roughly six rings are needed to “compete” with a simple trefoil knot. We attempt to quantify this finite knot-size effect.

In the absence of an exact statistical treatment of knotted polymers, several researchers have employed

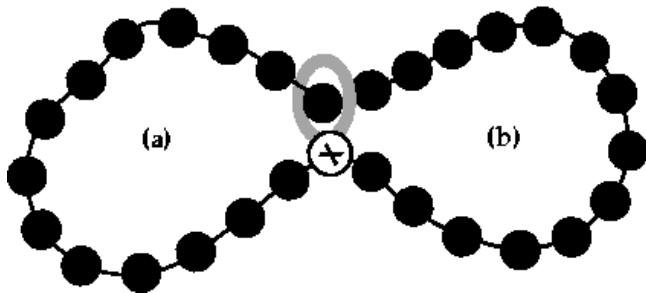


FIG. 2: A schematic depiction of two loops in competition. Sides (a) and (b) do not interact with each other. The position of one bead is always fixed (the one with X inside). The oval ring shows the position of the ‘hole’ separating the spaces in which the segments exist.

‘slip-links’ for gaining analytical insights on topological constraints[12, 13]. Slip-links can be envisioned as belt-buckles which force two points of the chain to be close to each other. Para-knots are collections of such slip-links, and have been proposed as means of designing entropy-driven functional molecules which are linked to each other mechanically rather than chemically[14]. In Sec. V, we also employ a para-knot model to explore the effects of a sub-leading scale on entropic competition.

## II. METHOD

We start by calculating the entropic exponents of a closed loop. Our model polymer consists of  $L$  hard spheres of diameter  $D$  connected into a chain by tethers which have no additional energy cost [15], but restrict the distance between connected spheres to be smaller than  $1.2D$ ; this prevents the chain from crossing itself. Figure 2 provides a schematic depiction of the simulation: Solid circles represent monomers of the chain; the position of one monomer (labeled with an X) is fixed in space, and the chain is forced to pass through a hole which is depicted by an oval ring in Fig. 2. The effect of the hole combined with the fixed monomer is to create two loops of lengths  $\ell$  and  $L - \ell$ . The two loops do not interact with each other: as soon as a monomer passes through the hole, it ceases to interact with the monomers of its previous side and starts to interact with the ones in the new side. In order to preserve the topology of each loop, we allow the monomers immediately adjacent to the hole on either side to interact with each other, and also allow the fixed monomer to interact with all the other monomers. It is also necessary to keep the hole narrow enough not to let knots pass through it (for later applications). The hole creates a barrier which slows down the process of transferring the chain from one side to the other. In fact, this entropic barrier is the major obstacle to the computation of the probability distribution of long chains ( $L > 300$ ) within a reasonable amount of CPU time. Obviously, this barrier depends on the en-

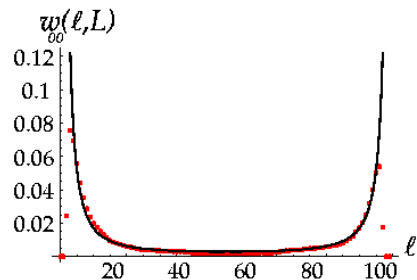


FIG. 3: Probability distribution for two loops exchanging monomers. The dots are the results of the simulation for  $10^9$  MC steps, with  $L = 100$ . The graphs are normalized such that the integrated weight is equal to one.

tropic exponents, and is less significant for a hole on a rigid wall. In calculating the exponent  $\gamma_{11}$  [8], we remove the entropic barrier (hole) completely; the two segments on the two sides of the wall can exchange monomers at any point on the wall (Fig. 1e). In this case, we let the monomers pass through the wall only based on their order along the chain, *i.e.*, monomer  $n$  can pass through the wall, only if monomer  $n - 1$  has already moved to the other side of the wall.

The number of configurations of the system depicted in Fig. 2 is the product of number of configurations of each loop, and thus scales as

$$w_{00}(\ell, L - \ell) = A\mu^L \ell^{-\nu d} \times (L - \ell)^{-\nu d}, \quad (3)$$

where  $\ell$  is the number of monomers in one of the loops. (The absence of a knot or ring on each loop is denoted by the index pair 00.) Note that the  $\mu$  does not affect the  $\ell$ -dependence, and shall in fact be ignored henceforth. Although the passage through a worm-hole may appear unphysical in this context, our simulations produce the correct results for the two non-interacting self-avoiding loops which exchange monomers. Figure 3 shows the probability distribution for the segment length  $\ell$ . The dots are the result of the simulation for  $10^9$  MC steps [16]. The solid line corresponds to the Eq. (3) with  $\nu = 0.588$  at  $d = 3$ . The graphs in this figure and all the other figures are normalized such that the integrated weight is equal to one. The good match of simulation with Eq. (3) confirms that our method for computing the probability distribution is accurate. Similar curves were produced through simulations for chains with different sizes  $L = 50$ ,  $L = 150$ , and  $L = 200$ ; all follow Eq. (3).

## III. SLIDING RINGS

To further examine the validity of our method, in this section we present results of simulations including *sliding rings*. For each configuration of a loop of length  $\ell$ , a sliding ring can occupy  $\ell$  different positions, and thus the probability distribution of such a loop scales as,  $w_1 \simeq \ell w_0 \sim \mu^\ell \ell^{-\nu d + 1}$ . In simulations, the passage of a chain

through the hole is stopped if a ring is placed exactly on the monomer entering the pore. Instead of simulating a “real” sliding ring, we calculate the probability that a ring might be sitting adjacent to the hole and then prevent the chain from passing through the hole with this probability. If we have one ring, the probability of the ring to be exactly on the monomer entering the hole is  $1/\ell$ . In case of many rings, this probability goes up.

We start by placing a ring on one of the loops of Fig. 2 and then we measure the histogram of lengths. Figure 4 shows the probability distribution of the loop side with one sliding ring. The increased entropy of the segment on which the ring is sliding biases the amount of time monomers spend on that side. The solid line in Fig. 4 corresponds to  $w_{10}(\ell, L) = A\ell/(\ell^{1.76}(L - \ell)^{1.76})$ . Note that this functional form is still singular at  $\ell \rightarrow 0$ , although the singularity is weakened compared to the case without the sliding ring. This singularity is not visible in Fig. 2, presumably due to the short size of the simulated chains.

The entropic effects can be increased even further by placing more sliding rings on the loops of Fig. 2. The presence of  $n$  sliding-rings on a loop enhances the number of configurations to

$$w_n \sim \frac{\ell!}{(\ell - n)!n!} w_0. \quad (4)$$

The side with the larger number of sliding rings is expected to dominate in a competition. Figure 5 shows the probability distribution when we have one ring on *each* side. The solid line in Fig. 5 corresponds to the formula,

$$w_{nn}(\ell, L) = A \frac{\ell!(L - \ell)!}{(\ell - n)!(L - \ell - n)!\ell^{1.76}(L - \ell)^{1.76}}, \quad (5)$$

with  $n = 1$ . The dots on the figures are the result of a simulation of  $10^9$  MC steps. Similar results have been observed for chains with sizes  $L = 50, 150,$  and  $200$ . The corresponding results with two rings on each side are shown in Fig. 6; the solid line represents Eq. (5) with  $n = 2$ . Note the dramatic difference between the shapes of these two figures: with one ring on each side the distribution is peaked (in fact singular) at the two extremes, while for  $n = 2$ , the maximum has moved to the center. This trend becomes even more pronounced in Fig. 7 which illustrates the case with  $n = 4$ . Clearly, increasing the number of rings results in a probability distribution which peaks more sharply in the middle. The solid line in Fig. 7 again represents Eq. (5) with  $n = 4$ . The good matches between the probability distributions obtained in simulations, and Eq. (5) for different numbers of rings  $n$  lend further credence to the validity of our method.

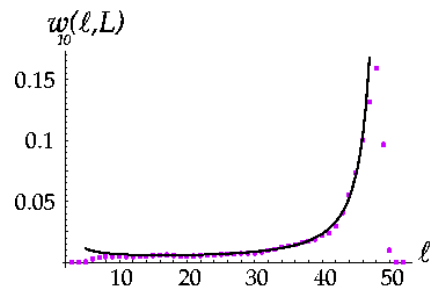


FIG. 4: Probability distribution of the size  $\ell$  of a loop with one sliding ring, in competition with a simple loop. The dots are the result of a simulation with over  $10^9$  MC steps for  $L = 50$ .

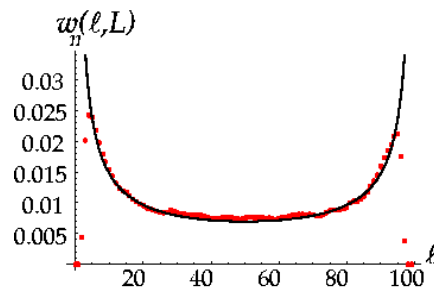


FIG. 5: Probability distribution of length for two loops with one ring on each side ( $L = 100$ ).

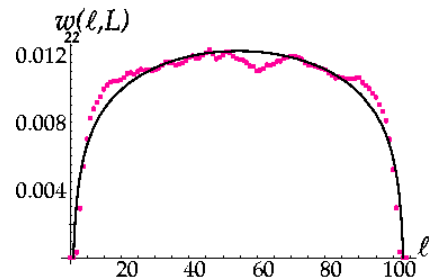


FIG. 6: Probability distribution for two loops with two rings on each side ( $L = 100$ ).

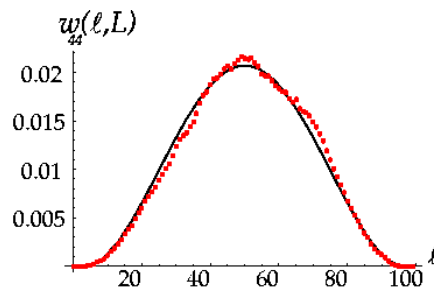


FIG. 7: Probability distribution for two loops with four rings on each side ( $L = 100$ ).

## IV. KNOTS

### A. Background

We are now in position to apply the entropic competition method to the more complicated problem of knots. Knots frequently appear in closed polymers and play a major role in numerous biological systems. For example, during transcription of DNA, a variety of “de-knotting” enzymes, called topoisomerases, remove knots and entanglements to allow this process to go forward[17, 18]. Understanding of the action of these enzymes has been improved with the help of knot theory. Knotted configurations have also been observed in some proteins and interfere with their folding into the proper shapes and thus lead to diseases, such as Alzheimer’s and primary amyloidosis[19]. While knotted configurations hamper the proper functioning of a number of biological and chemical systems, they have crucial and positive roles in many others. The tertiary structure of RNA is an example in which the topological entanglements may have positive influences. There has been extensive research on predicting and understanding the relation between structure and function in RNA [20]. The folded structure of some types of RNA molecules (Ribozymes) determine their catalytic activities which are crucial to the functioning of the cell[17]. Pseudo-knots, which are formed by base pairing between a loop and some region outside the loop, have been found in various kinds of RNAs and are recognized as simple RNA folding motifs[21]. A more physical example is provided by permanent entanglements in rubber, which restrict the number of allowed configurations of each segment, and thus influence the elasticity of rubber[22].

On the experimental front, artificial knots have been tied on both DNA and actin filaments [23], and the first Borromean DNA rings have also been assembled[24]. Single molecule techniques have provided a powerful tool to examine a wide variety of physical properties of knotted polymers [25]. Despite all this progress, our knowledge about the typical conformations and physical properties of knotted polymers remains rudimentary. This is due to the difficulty of incorporating topological constraints in the analytical treatments of the statistics of polymers, as mathematical methods of knot detection are mainly of “algorithmic” nature.[26]. This complexity has encouraged the use of Monte Carlo simulations, such as the one reported here.

### B. Competing knots

How does the altered topology of a closed curve with a knot modify the number of available configurations? To investigate this issue, Orlandini *et al.*[6] performed grand canonical Monte Carlo simulations of SA polygons with a fixed knot type  $\mathcal{K}$ . In these simulations the length of the chain is not fixed, but the set of allowed moves is such

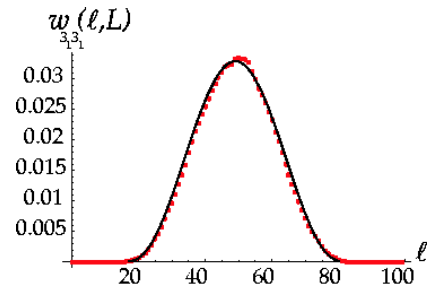


FIG. 8: Probability distribution for two loops with one knot on each side ( $L = 100$ ).

that the topology of the chain is preserved. Orlandini *et al.* conjectured that the number of configurations of knotted loops takes the same general form as Eq. (1), asymptotically behaving as

$$w_{\mathcal{K}} \sim A_{\mathcal{K}} \mu_{\mathcal{K}}^{\ell} \ell^{\alpha(\mathcal{K})-3}, \quad (6)$$

with parameters that may depend on the knot type  $\mathcal{K}$ . Assuming this form, one can find an expression for the mean length  $\langle n(\mathcal{K}) \rangle$ , a quantity that can be measured in the grand canonical simulations. Fitting the simulation data for  $\langle n(\mathcal{K}) \rangle^{-1}$ , and extrapolating the results to the limit of infinite size, Orlandini *et al.* can estimate the parameters in Eq. (6). In particular they confirm that the effective growth constant  $\mu_{\mathcal{K}}$  is independent of the knot type. Assuming that this is the case, they then conclude that the universal power-law exponents behave as  $\alpha(\mathcal{K}) = \alpha(\emptyset) + N_f$ , where  $\emptyset$  refers to a simple loop (unknot), while  $N_f$  is the number of prime factors in the knot type  $\mathcal{K}$ . Such a conclusion has a simple and elegant interpretation: each prime factor of the knot becomes a tight element that incorporates an asymptotically small fraction of the monomers. The tight factors can occupy any position along the remaining large loop, each increasing the number of configurations by a factor of roughly the size of the loop, much like the sliding rings discussed in the previous section.

If a prime knot, such as a trefoil, increases the number of configurations of the closed polymer by the same factor as a sliding ring, the two should behave similarly in the arena of “entropic competition.” Indeed a knotted loop added to one side of Fig. 2 pulls the entire chain on its side as in Fig. 4. However, when we place one trefoil knot on each of the loops, the resulting segment distribution, as plotted in Fig. 8 is qualitatively different from the curve found when a sliding ring appears on each side (Fig. 5). The distribution for the competing knots is peaked at the center, much like cases with more than one sliding ring on each side. The solid line in Fig. 5 in fact represents Eq. (5) with  $n = 4$ . We do not suggest that the trefoil is asymptotically similar to four rings, but that this is a good effective description of a trefoil knot with a few hundred monomers. To obtain more insight on finite-size effects, we compare the probability distributions of knotted loops with different sizes ranging from  $L = 50$  to

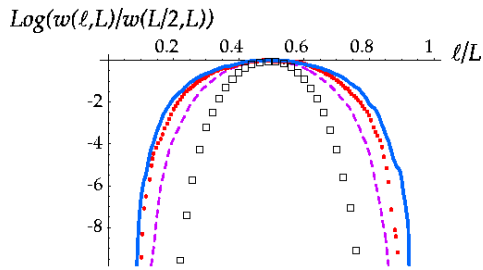


FIG. 9: A logarithmic plot of probability density for two loops with one knot on each side for  $N = 50$  (square), 100 (dashed line), 150 (dots), and 200 (solid line). The graphs were vertically displaced to coincide at  $\ell/L = 0.5$ . As  $L$  increases, the distributions become wider.

$L = 200$ .

Figure 9 shows the logarithmic plot of rescaled probability densities for  $N = 50, 100, 150$ , and 200, as a function of  $\ell/L$ . The  $y$  coordinates are shifted so that the maxima of distributions for all sizes coincide. We note that the maximum becomes flatter upon increasing  $L$ . The lack of data collapse is a clear indication of finite-size effects. To check this, we performed similar simulations with four rings on each side with chains of lengths  $L = 50$  through  $L = 200$ . In contrast to knots (Fig. 9), we observed that all rescaled curves collapsed in this case.

## V. KNOTS VERSUS RINGS

In order to compare the relative “strengths” of knots and rings in increasing the number of configurations, we performed several simulations in which we pitted a trefoil knot against different numbers of rings, as depicted in Fig. 10. While the hypothesis of a tight knot[6, 12, 27] suggests that the trefoil should be well matched to a single ring, in our simulations with chains of 100 monomers, we find that around 6 rings are necessary to prevent the chain from being pulled completely to the side with the trefoil. Part of this effect is no doubt due to the size of the knot: even in its most compact form the trefoil knot involves around 14 monomers, while the sliding ring is assumed to occupy only one. In actuality, even a ‘tight knot’ will most likely be considerably bigger than the minimal size, with typical sizes that grow with the length of the chain[28]. To test for these effects we performed some further studies as reported in this section.

To take account of the minimal size of the trefoil knot, we also added a similar constraint to the side with sliding rings. In these simulations the monomers were prevented to move from the ring side to the knot side with a probability of  $1/(\ell - 13)$ . This means that when  $\ell = 14$ , the monomer is strictly forbidden to pass through the hole from the ring side to the knot side; thus, at least 14 monomers remain on each side throughout the simula-

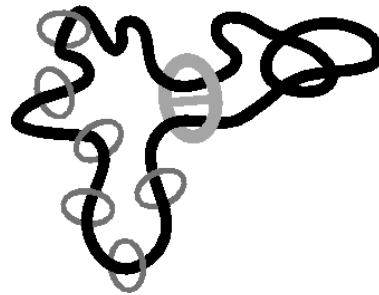


FIG. 10: Schematic “entropic competition” between a trefoil knot and 6 sliding rings.

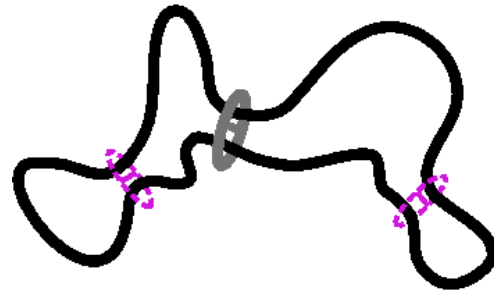


FIG. 11: Two loops are separated by the thick oval shaped hole. The dotted ovals are slip-links.

tion. Even in this case, we observe that the trefoil “wins” the competition against a single sliding ring. Once more, we found that at least four rings are need for the two sides of the chain to exert equal amount of force on each other. Thus the minimal size of the knot is not a crucial issue.

We certainly do not expect the trefoil to be maximally tight. The number of monomers participating in the knot region is itself a not-so-well-defined and fluctuating quantity. A better model than the sliding ring, which allows for this possibility, is the slip-linked para-knot depicted in Fig. 11. The thick oval ring in this figure represents the ‘worm-hole’ separating the two segments, while the dotted ovals are slip-links which keep two points on each loop close to each other (creating a figure-8 structure on each segment). The effect of each slip-link is similar to the hole in that they create two loops; however, there are self-avoiding interactions among all the monomers of a loop made into a figure-8 by the slip-link. The number of configurations of a figure-8 structure with self-avoiding constraints for  $1 \ll \ell \ll L$  scales as  $\ell^{-c}(L - \ell)^{-c}$  with  $c = 2.88$  in  $d = 2$  and  $c = 2.24$  in  $d = 3$  [29]. Although this formula is strictly valid only for large  $\ell$  and  $L$ , a recent experiment on a figure-8 chain on a vibrating plate in 2-dimensions is in good agreement with this formula[30, 31].

Extending the asymptotic formula for the figure 8 to all separations, we can obtain an analytic form for the number of configurations of two figure 8’s in competition. Assuming a minimal size  $s_{min}$  for each segment,



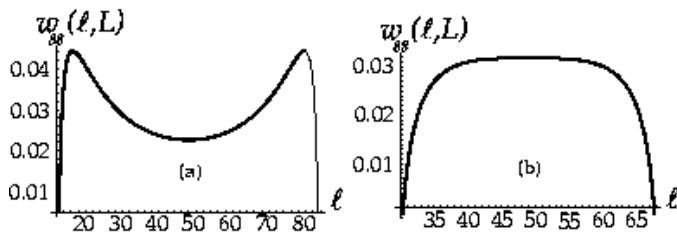


FIG. 12: Probability distribution for two loops with one slip-link on each side (figure-8), from Eq. (7) with  $L = 100$  and  $s_{min} = 14$  (a) and  $s_{min} = 30$  (b).

the number of configurations is

$$w_{8,8}(\ell, L) \simeq \int_{s_{min}}^{\ell} ds \frac{(\ell - s)}{s^c (\ell - s)^c} \times \int_{s_{min}}^{L-\ell} ds \frac{(L - \ell - s)}{s^c (L - \ell - s)^c}. \quad (7)$$

Each integrand represents the probability density of a loop with its associated para-knot. Since there exists self-avoiding interaction between each loop and its para-knot, we set  $c = 2.88$  and  $c = 2.24$  for two and three dimension respectively. Figure 12a is a graph of Eq. (7) with  $s_{min} = 14$  and  $c = 2.24$ . The distribution shown in Fig. 12a is qualitatively similar to the one in Fig. 5, for two loops with *one* sliding-ring on each side, in that for both cases, the minimum of the distributions is in the middle and their maxima are on the sides. If we increase the minimal size from  $s_{min} = 14$  to  $s_{min} = 30$ , the maximum moves to the middle as depicted in Fig. 12b.

## VI. CONCLUSIONS

An important quantity in polymer physics is the number of configurations that a chain of length  $\ell$  can take. As noted in the introduction, this quantity has the asymptotic form of  $\mu^\ell \ell^{-c}$  where  $\mu$  depends on the microscopic features of a chain while the exponent  $c$  is universal. In this paper we focus on obtaining the universal exponent, while bypassing the parameter  $\mu$ . To this end, we employ a hole (or buckle) to divide a polymer into two segments (see Figs. 1, 2), and then allow the two parts to exchange monomers and to “entropically” compete. The resulting histograms allow us to calculate the entropic exponents with a variety of boundary conditions and/or topological constraints.

The scaling form in Eq. 2 is only valid asymptotically, and there are in general corrections to scaling which complicate the extraction of entropic exponents for short polymers. In the application of entropic competition to knots, we find that finite size effects are so pervasive that we cannot extract reliable universal information pertaining to knots for ( $L < 300$ ). (We find an effective exponent of around 4 for a trefoil knot over the simulated lengths.) Indeed, simulations performed by Farago *et al.*[28] indicate that while the ratio of the knot size  $N_K$  to the total length of the chain decreases, the effective knot size grows with the size of the polymer, suggesting that simulations on very large chains are needed to avoid the finite size effect. An important question which remains is at what size of a molecule the universal predictions of the asymptotic theories are expected to hold.

The primary goal of this paper is to present the method of “entropic competition” for calculation of entropic exponents of polymers with different boundary conditions and under different topological constraints. Our procedure for extracting exponents is in principle simple, yet capable of producing accurate results. An intriguing application of the method to topologically constrained chains, such as knotted polymers, is also attempted in this paper. This example also illustrates the limitations of the technique, in that we find that finite-size effects are quite important to our simulated knotted chains with  $L < 300$  monomers.

It’s noteworthy to mention that each simulation reported in this paper was obtained in a maximum of two week’s CPU time on a desk-top computer. One can apply “entropic competition” method to longer chains and calculate “entropic exponents” with higher accuracy on a large cluster of computers with longer amounts of CPU time.

## VII. ACKNOWLEDGEMENTS

The authors would like to acknowledge helpful discussions with J. Rudnick, M. Deserno, and R. Metzler. This work was supported by NSF grant DMR-01-18213, and Israel Science Foundation Grant 38/02. RZ acknowledges support from the UC President’s Postdoctoral Fellowship program.

[1] P.-G. de Gennes, *Scaling concepts in polymer physics* (Cornell University Press, Ithaca, New York, 1979).  
 [2] K. F. Freed, *Renormalization group theory of macromolecules* (John Wiley & Sons, Inc. New York, 1987); J. des Cloizeaux and G. Jannink, *Polymers in solution: Their modeling and structure* (Clarendon Press, Oxford, 1990).

[3] S. B. Smith, L. Finzi, and C. Bustamante, *Science* **258**, 1122 (1992); S. B. Smith, Y. Cui, and C. Bustamante, *Science* **271**, 795 (1996); K. Svoboda, S. M. Block, *Ann. Rev. Biophys. Biomol. Structure* **23**, 247 (1994); A. Ashkin, *Proc. Natl Acad. Sci., USA* **94**, 4853 (1997); H. G. Hansma, *J. Vac. Sci. Technology* **B14**, 1390 (1995);  
 [4] A. Yu. Grosberg and A. R. Khokhlov, *Statistical Mechan-*

- ics of Macromolecules* (AIP Press, New York, 1994).
- [5] N. Madras and G. Slade, *The self-avoiding walk*, Birkhäuser, Boston (1993).
- [6] E. Orlandini, M. C. Tesi, E. J. Janse van Rensburg and S. G. Whittington, *J. Phys. A* **31**, 5953 (1998); and **29**, L299 (1996).
- [7] E. Gütter and E. Orlandini, *J. Phys. A* **32**, 1359 (1999).
- [8] K. De'Bell and T. Lookman, *Rev. Mod. Phys.* **65**, 87 (1993); E. Eisenriegler, K. Kremer, and K. Binder, *J. Chem. Phys.* **77**, 6296 (1982).
- [9] P. J. Park and W. Sung, *Phys. Rev. E* **57**, 730 (1998); M. Muthukumar, *Phys. Rev. Lett.* **86**, 3188 (2001); R. Zandi, D. Reguera, J. Rudnick, and W. M. Gelbart, *Proc. Natl Acad. Sci., USA* in press (2003).
- [10] N. L. Slack, M. Schellhorn, P. Eiselt, M. A. Chibbaro, U. Schulze, H. E. Warriner, P. Daidson, H. W. Schmidt and C. R. Safinya, *Macromolecules* **31**, 8503 (1998).
- [11] E. J. Janse van Rensburg and S. G. Whittington, *J. Phys. A* **24**, 3935 (1991)
- [12] R. Metzler, A. Hanke, P. G. Dommersnes, Y. Kantor and M. Kardar, *Phys. Rev. Lett.* **88**, 188101 (2002); *ibid* *Phys. Rev. E* **65**, 061103 (2002).
- [13] R. C. Ball, M. Doi, S. F. Edwards and M. Warner, *Polymer* **22**, 1010 (1981); P. G. Higgs and R. C. Ball, *Europhys. Lett.* **8**, 357 (1989); S. F. Edwards and T. A. Vilgis, *Polymer* **27**, 483 (1986).
- [14] R. Metzler and A. Hanke, *Chem. Phys. Lett.* **359**, 22 (2002).
- [15] Y. Kantor, M. Kardar, and D. R. Nelson, *Phys. Rev. Lett.* **57**, 791 (1986); and *Phys. Rev. A* **35**, 3056 (1987).
- [16] An elementary MC step consists of an attempt to move a randomly chosen sphere a distance less than  $0.15D$  in a random direction.  $L$  such attempts constitute one MC time unit.
- [17] B. Alberts, K. Roberts, D. Bray, J. Lewis, M. Raff and J. D. Watson, *The molecular biology of the cell* (Garland Science, New York, 1994).
- [18] C. R. Calladine and H. R. Drew, *Understanding DNA* (Academic Press, New York, 1997).
- [19] A. L. Fink, *Fold Des.* **3**, R9 (1998); V.N. Uversky, D. J. Segel, S. Doniach, and A. L. Fink, *Proc. Natl Acad. Sci., USA* **95**, 5480 (1998).
- [20] I. Tinoco Jr. and C. Bustamante, *J. Mol. Biol.* **293**, 271 (1999).
- [21] F. H. D. van Batenburg, A. P. Gulyaev, C. W. A. Pleij, J. Ng and J. Oliehoek, *Nucleic Acids Res.* **28**, 201 (2000); D. P. Giedroc, C. A. Theimer and P. L. Nixon, *J. Mol. Biol.* **298**, 167 (2000).
- [22] L. R. G. Treloar, *The physics of rubber elasticity* (Clarendon Press, Oxford, 1986); M. Doi and S. F. Edwards, *The theory of polymer dynamics* (Clarendon Press, Oxford, 1986).
- [23] Y. Arai, R. Yasuda, K. -I. Akashi, Y. Harada, H. Miyata, K. Kinoshita Jr. and H. Itoh, *Nature* **399**, 446 (1999);
- [24] C. Mao, W. Sun and N. C. Seeman, *Nature* **386**, 137 (1997).
- [25] V. V. Rybenkov, N. R. Cozzarelli, and A. V. Vologodskii, *Proc. Natl Acad. Sci., USA* **90**, 5307 (1993); S. Y. Shaw and J. C. Wang, *Science* **260**, 533 (1993).
- [26] L. H. Kauffman, *Knots and physics* (World Scientific, Singapore, 2001), 3rd ed.; A. C. C. Adams, *The knot book: an elementary introduction to the mathematical theory of knots* (Freeman, New York, 1994).
- [27] V. Katritch, W. K. Olson, A. Vologodskii, J. Dubochet and A. Stasiak, *Phys. Rev. E* **66**, 5545 (2000).
- [28] O. Farago, Y. Kantor, and M. Kardar, *Europhys. Lett.* **60**, 53 (2002).
- [29] B. Duplantier, *Phys. Rev. Lett.* **57**, 941 (1986).
- [30] M. B. Hastings, Z. A. Daya, E. Ben-Naim and R. E. Ecke, *Phys. Rev. E* **61**, 025102(R) (2002).
- [31] The experiment in Ref. [30] is done with a vibrated granular chain far from equilibrium. Nonetheless, their results are consistent with the theoretical equilibrium predictions.